Modified Local Updates of the Ant Colony Optimization Algorithm for Image Edge Detection

David
STMIK Pontianak, Pontianak, Indonesia
David@stmikpontianak.ac.id

Edy Victor Haryanto S
Universitas Potensi Utama, Medan, Indonesia
edyvictor@gmail.com

Febriana
STMIK Pontianak, Pontianak, Indonesia
febrianachen@stmikpontianak.ac.id

***Abstract*— Edge detection refers to the process of extracting edge information of an image. It is considered as a basic step used in the majority of image processing applications. The aim of this study was to modify local updates of pheromones. Therefore, the convergence of the Ant Colony Optimization (ACO) algorithm applied to image edge detection could be accelerated effectively. Such the algorithm is a metaheuristic method applying the ants as agents with their pheromone updates for an effective and efficient solution of search processes. Five ACO algorithms for edge detection, i.e., ACO, modified ACO, ACO with the Sobel operator, ACO with the Prewitt operator, and ACO with the Isotropic operator were in comparison. Nearly optimal solutions of several image datasets were discovered through examination of the number of ants and iterations. Additionally, calculation results of each image dataset and algorithm were compared. The evidence shows that solutions produced by all algorithms are equally good. For an image dataset with more ants, however, it is found that the modified ACO algorithm has the best solution in terms of time convergence. The study contribution is further next to adding the concept of improving edge detection in the image with the ant colony optimization algorithm. The implementation of the study carried out is to modify local updates which are functionally used for improving the edge detection dealt with by ants taking part in ACO.**

Keywords—Ant Colony Optimization, Edge Detection, Local Updates

I. Introduction

Researchers are greatly focusing on processing techniques of digital images. Numerous algorithms have been developed to optimize the results. One of the best techniques is preprocessing employed to facilitate the system in processing the digital images [1].

One of the algorithms currently being developed is swarm intelligence [2]. It is a biologically inspired computational algorithm on connectionism and social behavior [2,3]. It is further in relation to the field of artificial intelligence since the elements are widely associated with machine learning [4]. Swarm intelligence relies heavily on the fields of biology, computer science, and mathematics [4]. It is simply the improving use of computers in modeling the phenomena of life simultaneously. Biologically inspired computing is a major part of natural computation [2,3].

Ant Colony Optimization (ACO) becomes the focus of this research. It is a global optimization algorithm which is based on observation of the group behavior of ant colonies [5,6]. Based on the description, this algorithm can be developed mathematically. There are advantages and disadvantages of algorithms developed through swarm intelligence [7,8]. Some of them have high accuracy with sacrificed computational speed. Nonetheless, sacrificing the accuracy, the rest are great in processing the data quickly [7,8].

In this study, the ACO algorithm will be tested in performing the edge detection to find out its advantages and disadvantages [9]. This detection is the process of extracting edge information from an image [10]. Moreover, it is considered as a basic step used in most image processing applications [10,11]. An edge in an image can be regarded as a boundary between two dissimilar areas [10,11].

Numerous approaches have been used to perform image edge detection. Commonly used methods are Prewitt [12,13], Sobel [12], and Canny [12,14]. For this purpose, the latest research, however, is applying ACO [9], a heuristic method imitating the behavior of ants to solve discrete optimization problems [6,7,9]. Ants use special chemical compounds called pheromones to mark pathways between food sources and their colony [6,7]. These pathways are used by subsequent ants as a reference to search the food because pheromones increase the likelihood of paths being selected [6,7].

An initial concept of ACO is that the dispersal process of the first ants is carried out at random. It changes the pheromone level based on update rules of local pheromones [6,7]. This condition can lead to an imbalance of ant distribution, further affecting the path finding process and the rate of pheromone evaporation [15,16]. In the ACO system, the primary thing is the use of both global and local pheromone updates [16]. Several previous studies indicate that in comparison to local updates, the global ones can effectively expedite the ACO convergence [17]. Based on global search, the local one adjusts the optimal paths to avoid collisions in the local environment [18].

Researchers endeavored to propose modification of local pheromone updates in order to improve convergence. The ACO algorithm can be hybridized through edge detection operators such as Isotropic, Sobel, and Prewitt[21]. This study would show outcomes of performance of five compared algorithms for edge detection such as ACO, modified ACO, ACO with the Sobel operator, ACO with the Prewitt operator, and ACO with the Isotropic operator. Nearly optimal solutions of several image datasets were discovered through examination of the number of ants and iterations. Performance was examined through comparison of values of PNSR, MSE, SSIM, and PSNR generated by traditional ACO, ACO with operators, and the proposed ACO modification [22,23]. The planned way is thought to be effective in improving the original ACO if the PSNR value of the modified ACO algorithm is superior to the original ACO.

II. Methods

A. Research Stages

In this study, several stages consisting of image data retrieval, preprocessing, ACO parameter initialization, and edge detection (illustrated in Figure 1) were carried out.

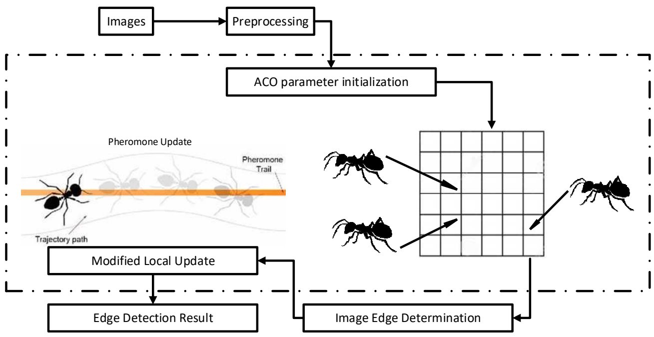

Fig. 1. Research Block Diagram

An early process was taking or selecting the images. Furthermore, they were preprocessed. After obtaining a gray image, edge detection was conducted by using the ACO method. Next, ACO initialization parameters were defined. The ACO algorithm would position the ant agents to pixel areas in images. The edge of images was determined by the ants. Another step was that each ant would update both global and local pheromones. In this study, modified ACO was proposed during local pheromone updates. A final result was images with edge detection.

B. Image Dataset

Data with colored objects, and the ones with gray colors and different dimensions were applied. Tested images were used as objects to examine methods in image processing (https://informatika.stei.itb.ac.id/~rinaldi.munir/Koleksi/Citra%20Uji/CitraUji.htm (accessed on 30 June 2022)

C. Preprocessing

A luminosity method was used to convert color images into gray images since its nature was closer to the perception of human vision [19]. The value of each color element (R=red, G=green, and B=blue) was computed through weight addition based on it [19,20]. Human vision was more sensitive to green. Hence, Element G had the highest weight in comparison to the others [19,20]. Input data used in the system was an RGB image transform into a gray image through the aforementioned method. The calculation of conversion of color images into gray images could be mathematically formulated as Equation 1 [20,25]:

$$\text{Grayscale} = 0.2989 * R + 0.587 * G + 0.114 * B \tag{1}$$

D. Ant Colony Optimization for Edge Detection

The strategy used to detect image edges was ACO. It is a nature-inspired optimization algorithm motivated by the foraging behavior of ants. They use special chemical compounds called pheromones to mark the pathways between the food source and their colony. Pheromone pathways are used by subsequent ants as a reference for food searches as pheromones increase the likelihood of paths being selected.

Initialization was conducted at the beginning of ACO process. In this step, the procedure was performed. Parameters used were the number of construction steps (L), iterations (N), the number of ants (K), pheromone evaporation rates (ρ), pheromone decay (φ), weighting factors of pheromones (α), and weighting factors of heuristic information (β). Ant journeys covered a number of construction steps. Ants would move in an image until the target number was established. In the construction process (nth), a number of ants (kth) would move from node (i) to node (j) following the movement probability ($Pi,j(n)$). A rule was shown in Equation 2 [9,24].

$$P_{i,j}^{(n)} = \frac{\left(\tau_{i,j}^{n-1}\right)^{\alpha} \left(\eta_{i,j}\right)^{\beta}}{\sum_{j \in \Omega_i} \left(\tau_{i,j}^{n-1}\right)^{\alpha} \left(\eta_{i,j}\right)^{\beta}}, \text{if } j \in \Omega_i \tag{2}$$

where:
$P_{i,j}^{(n)}$ = movement probability
α = weighting factor of pheromones
β = weighting factor of heuristic information
□□ = the neighboring node of ants given to node (i)
□ = pheromone updates
η = heuristic information

Moreover, construction solutions becoming additional measures were carried out before updating the pheromone values. Achieving the success of this process was impossible if only an ant was engaged. Pheromones were then renewed globally (global pheromone updates) and locally (local pheromone updates). The latter were conducted each time construction steps were taken. Here pheromones were damaged (pheromone decay). This aimed to reduce the concentration of pheromones at edges traversed. Equation 3 represented local pheromone updates [9,24].

$$\tau_{i,j} = (1 - \varphi)\tau_{i,j} + \varphi\tau_o \tag{3}$$

where:
φ = pheromone decay
□ = pheromone updates

The goal of improving the proposed algorithms with local pheromone updates was to solve edge detection problems. It was influenced by some ant agents becoming the solutions to the problems of determining the image edges traced through those traversed. This research, thus, suggested that evaporation rates were stochastically added through provision of a small random value divided by the number of ant agents. Proposed local pheromone updates were shown in Equations 4 and 5.

$$\tau_{i,j} = \Delta f + (1 - \varphi)\tau_{i,j} + \varphi\tau_o \tag{4}$$

where:

$$\Delta f = \frac{random(\rho)}{\kappa} \tag{5}$$

ρ = pheromone evaporation rates
K = number of ants

A principal contribution of proposed local update strategy was to use the ACO algorithm to optimize pheromone evaporation so that performance of determining ACO edges became achievable. Each ant agent moved through pheromone trails by using algorithm rules and this process continued until edge determination criteria were met.

Global pheromone updates were, nonetheless, carried out after maximal construction steps in iterations were wholly taken. Here pheromone evaporation occurred. Respective updates of pheromones were shown in Equation 6 [9,24].

$$\tau_{i,j} = (1-\rho)\tau_{i,j} + \rho\Delta\tau_{i,j} \qquad (6)$$

where:

ρ = pheromone evaporation rates

$\Delta\tau_{i,j}$= a total of pheromones for global pheromone updates

There were movement rules of ACO with probability factors at eight neighboring pixels. Matrices of movement probability were calculated. Pixels with maximal probability factors in detecting the neighborhood had edges. In order to reduce repeated movement, stopping criteria rules were applied. Specifically, it stopped after paths (by any of the ants) and all the eight neighboring pixels (by all ants) happened [9]. Figure 2 showed the movement rules.

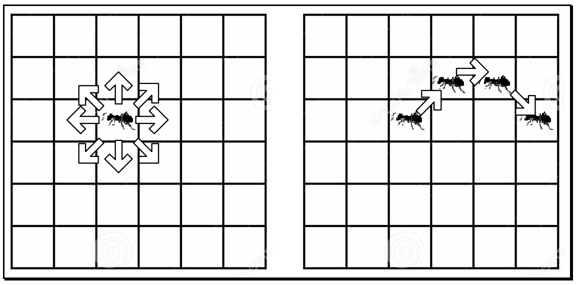

Fig. 2. Movement Rules of Ants [9]

Ant distribution was determined based on gradient values indicating the presence of edges in an area. Gradients were formed by gradual transitions or color changes [9]. In image processing, derivative-based operators became the basis of computation, for example Sobel, Prewitt, Canny, and Robert [9,21]. Ants occupying the pixel positions based on gradients whose values were greater than or equal to the threshold would move to eight neighboring pixels to determine edges. Neighboring relationships of pixels could be seen in Figure 3.

$I_{i-1,j-1}$	$I_{i-1,j}$	$I_{i-1,j+1}$
$I_{i,j-1}$	I	$I_{i,j+1}$
$I_{i+1,j-1}$	$I_{i+1,j}$	$I_{i+1,j+1}$

Fig. 3. Neighboring Relationships of Pixels

The relationships showed intensity values representing each image pixel. Besides, heuristic information ($\eta_{i,j}$) was obtained through Equation 7.

$$\eta_{i,j} = \frac{max_{i,j}\begin{pmatrix}|I(i-1,j-1)-I(i+1,j+1)|,|I(i-1,j+1)-I(i+1,j-1|, \\ |I(i,j-1)-I(i,j+1)|,|(i-1,j)-I(i+1,j)|\end{pmatrix}}{\eta_{max}} \qquad (7)$$

where:

η_{max}= maximal heuristic value

Each ant moving at random would produce q whose values were in the range from 0 to 1. If q was greater than q0, movement rules were applied. However, if q was less than q0, ants should move based on transitions maximizing the pheromone update values $(\tau_{i,j})^{\alpha}$ and heuristic information $(\eta_{i,j})^{\beta}$. The movement on pixels of Row i and Column j (Pi,j) was equal to multiplication of pheromones α and heuristic information β divided by multiplication of eight neighborhood areas.

For the edges with ACO, a threshold of the final pheromone matrix τ^{N} was used. Pixels could then be claimed as edges or not. In this proposed study, the threshold value (T) was obtained through the otsu method [25] determining the best solutions based on the number of pheromones stored in each pixel. Also, it reduced produced gray images into binary images with two possible values of pixels. An initialized threshold T(0) was selected based on the average of pheromone matrix values as in Equation 8.

$$T^{(0)} = \frac{\sum_{i=1}^{x}\sum_{j=1}^{y}\tau_{i,j}^{(N)}}{x.y} \qquad (8)$$

where:
x = image width
y = image height

Fitness values determining whether pixel became edges ($E_{i,j} = 1$) or not ($E_{i,j} = 0$) were calculated by using Equation 9.

$$E_{i,j} = \begin{Bmatrix}1, & if\,\tau_{i,j}^{(N)} \geq T^{(l)} \\ 0, & other\end{Bmatrix} \qquad (9)$$

where:
T = threshold
N = iteration
l = iteration index

III. EXPERIMENTAL RESULTS

In terms of implementation and examination, the specification of hardware used was 2.5 GHz Intel(R) Core (TM) i5-7200U processor with Turbo 2.7GHz, 12GB memory capacity. Meanwhile, software used in this study was the Python programming language with Anaconda tools.

Examination was conducted to cognize system performance of detecting the image edges. These cover the number of iterations and process time based on the number of ants. Values of PNSR, MSE, SSIM, and RSME produced through traditional ACO, ACO with operators, and proposed and modified ACO were compared.

In this study, initial examination on the number of iterations (respectively 2, 10, 50, 100, and 500) was carried out to obtain the optimal one that would be used in the scenarios. The focus was on the modified ACO method. The first test scenario involved the number of construction steps (L = 50), iterations (N = 10), the number of ants (K = 100), pheromone evaporation rates (ρ = 0.05), pheromone decay (φ = 0.1), weighting factors of pheromones (α = 1.0), weighting factors of heuristic information (β = 2.0), initial pheromones = 0.1, and threshold (T = 0.6). Examination results for the number of iterations of the modified ACO method was shown in Figure 4.

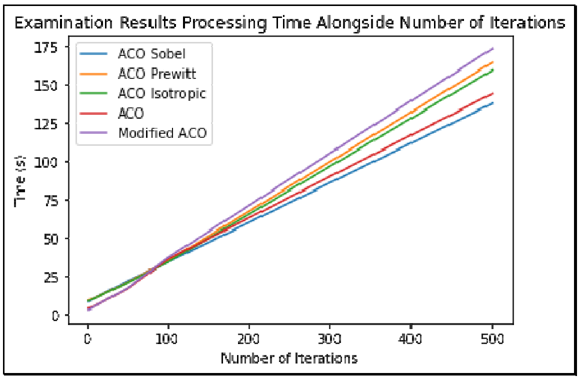

Fig. 4. Examination Graphic of the Number of Iterations

Referring to trial outcomes of the number of iterations through the modified ACO method, it was found that the more the number of iterations was, the better the edge detection results became in terms of sharpness and thickness (see Figure 5).

(a) Lena Image

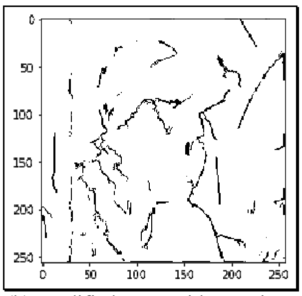

(b) Modified ACO with Iterations =2

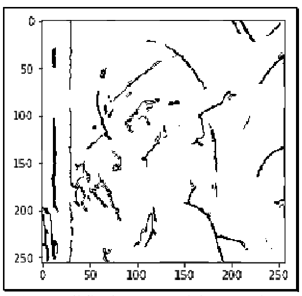

(c) Modified ACO with Iterations =10

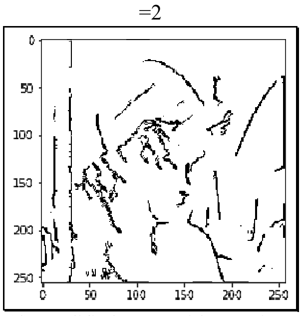

(d) Modified ACO with Iterations =50

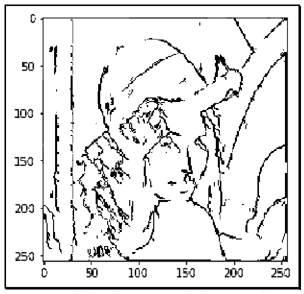

(e) Modified ACO with Iterations =100

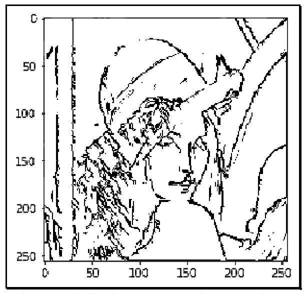

(f) Modified ACO with Iterations =500

Fig. 5. Image of Edge Detection Utilizing the Modified ACO Algorithm with the Number of Ants (K = 100)

The second examination was conducted to measure the performance of processing time based on the number of ants through all ACO algorithms. Lena image was in use. The parameter involved the number of construction steps (L = 50), iterations (N = 10), the number of ants (K = 1000), pheromone evaporation rates (ρ = 0.05), pheromone decay (φ = 0.1), weighting factors of pheromones (α = 1.0), weighting factors of heuristic information (β = 2.0), initial pheromones = 0.1, and threshold (T = 0.6). Figure 6 revealed images of edge detection with the number of ants (k = 1000). Nevertheless, examination results with the number of iterations of the modified ACO were represented in Figure 7.

(g) Lena Image

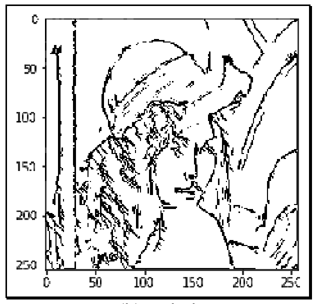

(h) Sobel

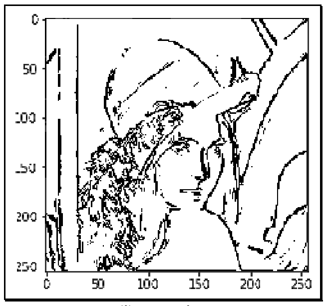

(i) Prewitt

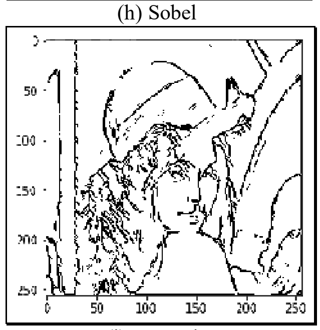

(j) Isotropic

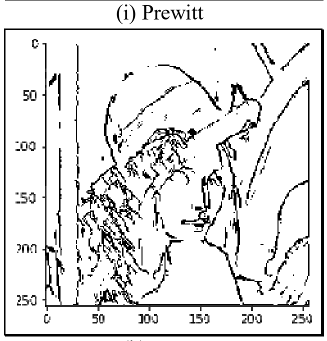

(k) ACO

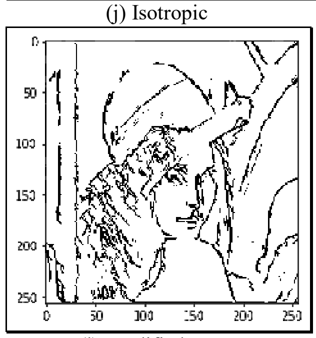

(l) Modified ACO

Fig. 6. Images of Edge Detection with the Number of Ants (K = 1000)

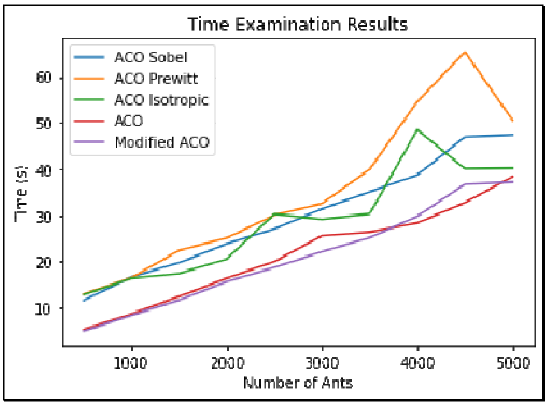

Fig. 7. Time Examination Results

The third trial scenario was performed to cognize the performance of all ACO algorithms based on edge detection results of dataset images. There were 15 images tested. The parameter included the number of ants (K = 500), the number of construction steps (L = 50), iterations (N = 2), pheromone evaporation rates (ρ = 0.05), pheromone decay (φ = 0.1), weighting factors of pheromones (α = 1.0), and weighting factors of heuristic information (β = 2.0), initial pheromones = 0.1 and threshold (T = 0.6) existed in Table 1.

TABLE I. EXAMINATION TABLE

No	Image	Algorithm	PSNR	SSIM	MSE	RMSE
1	Lena (256 x 256)	ACO Sobel	5.932	0.177	105.167	128.812
		ACO Prewitt	5.909	0.195	105.396	129.15
		ACO Isotropic	5.914	0.192	105.316	129.068
		ACO	5.898	0.192	105.168	129.319
		Modified ACO	5.905	0.193	105.227	129.211
2	Lena (512 x 512)	ACO Sobel	5.649	0.219	105.605	133.076
		ACO Prewitt	5.594	0.241	105.481	133.925
		ACO Isotropic	5.621	0.235	105.576	133.508
		ACO	5.623	0.241	105.572	133.471
		Modified ACO	5.623	0.237	105.52	133.465
3	Baboon (412 x 512)	ACO Sobel	6.048	0.061	106.659	127.101
		ACO Prewitt	5.951	0.065	106.596	128.525
		ACO Isotropic	6.021	0.061	106.556	127.492
		ACO	6.026	0.062	106.85	127.42
		Modified ACO	5.996	0.062	106.705	127.862
4	Barbara (512 x 512)	ACO Sobel	5.347	0.118	106.571	137.784
		ACO Prewitt	5.265	0.125	106.684	139.096
		ACO Isotropic	5.28	0.116	106.502	138.853
		ACO	5.301	0.125	106.498	138.519
		Modified ACO	5.287	0.126	106.522	138.732
5	Bird (256 x 256)	ACO Sobel	5.803	0.376	119.511	130.74
		ACO Prewitt	5.761	0.39	119.803	131.365
		ACO Isotropic	5.772	0.386	119.522	131.194
		ACO	5.767	0.389	119.759	131.278
		Modified ACO	5.774	0.39	119.819	131.171
6	Boat (512 x 512)	ACO Sobel	6.39	0.2	113.883	122.186
		ACO Prewitt	6.369	0.209	114.078	122.489
		ACO Isotropic	6.342	0.202	114.203	122.866
		ACO	6.339	0.206	114.008	122.917
		Modified ACO	6.3	0.204	114.154	123.461
7	Camera (256 x 256)	ACO Sobel	5.279	0.25	112.676	138.866
		ACO Prewitt	5.191	0.254	112.242	140.279
		ACO Isotropic	5.222	0.251	112.503	139.771
		ACO	5.219	0.254	112.54	139.834
		Modified ACO	5.234	0.255	112.71	139.589
8	Circles (256 x 256)	ACO Sobel	3.057	0.283	149.937	179.347
		ACO Prewitt	3.056	0.283	149.878	179.356
		ACO Isotropic	3.057	0.283	150.026	179.342
		ACO	3.056	0.283	149.869	179.366
		Modified ACO	3.055	0.283	149.858	179.385
9	Goldhill (256 x 256)	ACO Sobel	5.597	0.053	105.988	133.866
		ACO Prewitt	5.355	0.067	105.773	137.655
		ACO Isotropic	5.47	0.062	105.6	135.84
		ACO	5.413	0.063	105.735	136.732
		Modified ACO	5.44	0.064	105.681	136.321
10	Girl (256 x 256)	ACO Sobel	8.082	0.226	95.539	100.565
		ACO Prewitt	8.211	0.252	95.01	99.079
		ACO Isotropic	8.166	0.235	95.329	99.597
		ACO	8.191	0.245	95.105	99.306
		Modified ACO	8.206	0.242	95.1	99.134
11	Girl (256 x 256)	ACO Sobel	7.525	0.205	94.377	107.218
		ACO Prewitt	7.581	0.228	94.067	106.539
		ACO Isotropic	7.571	0.219	94.117	106.659
		ACO	7.582	0.222	94.041	106.528
		Modified ACO	7.59	0.223	94.134	106.428
12	Peppers (512 x 512)	ACO Sobel	4.445	0.154	105.341	152.854
		ACO Prewitt	4.429	0.167	105.526	153.139
		ACO Isotropic	4.424	0.169	105.495	153.226
		ACO	4.41	0.17	105.457	153.471
		Modified ACO	4.418	0.166	105.33	153.333
13	Slope (256 x 256)	ACO Sobel	5.11	0.361	93.353	141.592
		ACO Prewitt	5.117	0.363	93.384	141.48
		ACO Isotropic	5.111	0.362	93.366	141.572
		ACO	5.113	0.362	93.38	141.547
		Modified ACO	5.115	0.363	93.4	141.518
14	Text (256 x 256)	ACO Sobel	7.368	0.107	157.487	109.181
		ACO Prewitt	7.339	0.104	157.695	109.545
		ACO Isotropic	7.37	0.107	157.96	109.149
		ACO	7.391	0.109	158.185	108.896
		Modified ACO	7.399	0.111	158.434	108.789
15	Zelda (512 x 512)	ACO Sobel	3.992	0.167	104.16	161.04
		ACO Prewitt	3.932	0.176	104.282	162.15
		ACO Isotropic	3.972	0.168	104.258	161.412
		ACO	3.94	0.174	104.181	162.008
		Modified ACO	3.929	0.174	104.171	162.206

Finally, examination was conducted to find out the values of RMSE, SSIM, MSE, and PSNR and determine the system performance of ACO in detecting the image edges. The ones of PSNR and MSE generated through all ACO algorithms and the proposed ACO were compared. PSNR indicated comparative relationships between maximal values and noise, the result accuracy. High PSNR values showed that edge detection was generated better (see Table 1). Outcomes of SSIM were, however, decimals between 0 and 1. Getting closer to 1, images had proximity to the original ones. As a consequence, when SSIM values were getting close to zero, edge detection was good. Table 1 provided evidence that such values were very good in terms of interrelated ACO algorithms. Greater RMSE values led to greater error rates. With reference to Table 1, they were good in terms of interrelated ACO algorithms.

CONCLUSION

Based on research test results, it can be concluded that by using the ACO algorithm, it is possibility for the system to detect object edges. There is rapid edge detection system generated throughout modified ACO. In this case, it outperforms traditional ACO. Nonetheless, it is comparable to ACO using operators for various test images. This condition is indicated by higher PSNR values. The study contribution is further next to adding the concept of improving edge detection in the image with the ant colony optimization algorithm. The implementation of the study carried out is to modify local updates which are functionally used for improving the edge detection dealt with by ants taking part in ACO. For future research, it is necessary to improve the ant distribution and regulate ant movement to determine neighboring pixels at random, for example by adjusting the levels of neighboring gradients.

REFERENCES

[1] M. Gandhi, J. Kamdar, & M. Shah. "Preprocessing of Non-symmetrical Images for Edge Detection". *Augmented Human Research*, 5(1), 1-10. 2020.

[2] J. Tang, G. Liu, & Q. Pan. "A Review on Representative Swarm Intelligence Algorithms for Solving Optimization Problems: Applications and Trends". *IEEE/CAA Journal of Automatica Sinica*, 8(10), 1627-1643. 2021.

[3] M. Sotomayor, J. D. Pérez-Castrillo, & F. Castiglione. "*Complex Social and Behavioral Systems: Game Theory and Agent-based Models*". Springer Nature. 2020.

[4] K. Kaur & Y. Kumar. "Swarm Intelligence and Its Applications towards Various Computing: A Systematic Review". In 2020 *International Conference on Intelligent Engineering and Management (ICIEM)* (pp. 57-62). IEEE. 2020.

[5] A. Swarnkar & A. Swarnkar. "Artificial Intelligence-based Optimization Techniques: A Review". *Intelligent Computing Techniques for Smart Energy Systems*, 95-103. 2020.

[6] H. Zhao & C. Zhang. "An Ant Colony Optimization Algorithm with Evolutionary Experience-guided Pheromone Updating Strategies for Multi-objective Optimization". *Expert Systems with Applications*, 201, 117151. 2022.

[7] X. Zhou, H. Ma, J. Gu, H. Chen & W. Deng. “Parameter Adaptation-based Ant Colony Optimization with Dynamic Hybrid Mechanism”. *Engineering Applications of Artificial Intelligence*, 114, 105139. 2022.

[8] M. N. Sadiku & S. M. Musa. “*Swarm Intelligence in a Primer on Multiple Intelligences*”. (pp. 211-222). Springer, Cham. 2021.

[9] A. Kumar & S. Raheja. “Edge Detection Using Guided Image Filtering and Enhanced Ant Colony Optimization”. *Procedia Computer Science*, 173, 8-17. 2020.

[10] B. K. Shah, V. Kedia, R. Raut, S. Ansari & A. Shroff. “Evaluation and Comparative Study of Edge Detection Techniques”. *IOSR Journal of Computer Engineering*, 22(5), 6-15. 2020.

[11] Y. Jin & W. Wei. “Image Edge Enhancement Detection Method of Human-computer Interaction Interface Based on Machine Vision Technology”. *Mobile Networks and Applications*, 1-9. 2022.

[12] T. Peng-o & P. Chaikan. “High Performance and Energy Efficient Sobel Edge Detection”. *Microprocessors and Microsystems*, 87, 104368. 2021.

[13] S. R. Biswal, T. Sahoo & S. Sahoo. “Prediction of Grain Boundary of a Composite Microstructure Using Digital Image Processing: A Comparative Study”. *Materials Today: Proceedings*, 41, 357-362. 2021.

[14] L. Wang, X. Gu, Z. Liu, W. Wu & D. Wang. “Automatic Detection of Asphalt Pavement Thickness: A Method Combining GPR Images and Improved Canny Algorithm”. *Measurement*, 196, 111248. 2022.

[15] S. Mateusz, S. Grazyna, B. Aleksander & T. Wojciech. “Distributed Ant Colony Optimization Based on Actor Model”. Parallel Computing, 90, 102573. https://doi.org/10.1016/j.parco.2019.102573. 2019.

[16] F. Stefka. “Ant Colony Optimization and Applications”. *Springer*, Cham, 3-8. 2021.

[17] Y. Kang, Y. Xiaoming, L. Shen, & P. Han. “A Novel Ant Colony Optimization Based on Game for Traveling Salesman Problem”. *Applied Intelligence* 50.12: 4529-4542. 2020.

[18] S. Qi, Z. Qinglei, W. Shuxin, L. Qiang, & C. Xiaohe. “Dynamic Path Planning for Unmanned Vehicles Based on Fuzzy Logic and Improved Ant Colony Optimization." *IEEE Access 8*: 62107-62115. 2020.

[19] K. D. Avadhesh, K. Y. Rakesh, & M. Ramapati. “Image Contrast Optimization Using Local Color Correction and Fuzzy Intensification”. *International Journal of Advanced Computer Science and Applications*, 12(5). 2021.

[20] U. Garay, E. Pérez, J. Casanova, & M. Kratohvil. “Color Intensity, Luminosity, Contrast and Art Prices: The Case of Jean-Michel Basquiat”. *Academia Revista Latinoamericana de Administración*. 2022.

[21] B. Dhruv, N. Mittal, & M. Modi. "Early and Precise Detection of Pancreatic Tumor by Hybrid Approach with Edge Detection and Artificial Intelligence Techniques". *EAI Endorsed Transactions on Pervasive Health and Technology*, 7(28), e1-e1. 2021.

[22] U. Sara, M. Akter, & M. S. Uddin. "Image Quality Assessment through FSIM, SSIM, MSE and PSNR—A Comparative Study". *Journal of Computer and Communications*, 7(3), 8-18. 2019.

[23] A. L. Ramos, J. Domingo & D. P. Y. Barfeh. "Analysis of Weiner Filter Approximation Value Based on Performance of Metrics of Image Restoration". *In 2020 International Conference on Electrical, Communication, and Computer Engineering (ICECCE)* (pp. 1-6). IEEE. 2020.

[24] W. Gao. "New Ant Colony Optimization Algorithm for the Traveling Salesman Problem". *International Journal of Computational Intelligence Systems*, 13(1), 44-55. 2020.

[25] F. Liantoni, N. F. Rozi, T. Indriyani, W. M. Rahmawati, & R. K. Hapsari. "Gradient-based Ant Spread Modification on Ant Colony Optimization Method for Retinal Blood Vessel Edge Detection". *In IOP Conference Series: Materials Science and Engineering* (Vol. 1010, No. 1, p. 012021). IOP Publishing. 2021.